Published in final edited form as:

J Am Chem Soc. 2023 May 31; 145(21): 11735–11744. doi:10.1021/jacs.3c02273.

Fenton-like Chemistry by a Copper(I) Complex and H_2O_2 Relevant to Enzyme Peroxygenase C–H Hydroxylation

Bohee Kim,
Department of Chemistry, The Johns Hopkins University, Baltimore, Maryland 21218, United States

Magdalene T. Brueggemeyer,
Department of Chemistry, Stanford University, Stanford, California 94305, United States

Wesley J. Transue,
Department of Chemistry, Stanford University, Stanford, California 94305, United States

Younwoo Park,
Department of Emerging Materials Science, Daegu Gyeongbuk Institute of Science and Technology, (DGIST), Daegu 42988, Republic of Korea

Jaeheung Cho,
Department of Chemistry, Ulsan National Institute of Science and Technology (UNIST), Ulsan 44919, Republic of Korea

Maxime A. Siegler,
Department of Chemistry, The Johns Hopkins University, Baltimore, Maryland 21218, United States

Edward I. Solomon,
Department of Chemistry, Stanford, University, Stanford, California 94305, United States

Kenneth D. Karlin
Department of Chemistry, The Johns, Hopkins University, Baltimore, Maryland 21218, United States

Corresponding Authors **Edward I. Solomon** – edward.solomon@stanford.edu, **Kenneth D. Karlin** – karlin@jhu.edu.

Author Contributions

The manuscript was written through contributions of all authors. All authors have given approval to the final version of the manuscript.

ASSOCIATED CONTENT

Supporting Information

The Supporting Information is available free of charge at https://pubs.acs.org/doi/10.1021/jacs.3c02273.

Experimental details, characterization data, and X-ray crystallographic data for [**3**]$B(C_6F_5)_4$ (PDF)

Accession Codes

CCDC 2245700 contains the supplementary crystallographic data for this paper. These data can be obtained free of charge via www.ccdc.cam.ac.uk/data_request/cif, or by emailing data_request@ccdc.cam.ac.uk, or by contacting The Cambridge Crystallographic Data Centre, 12 Union Road, Cambridge CB2 1EZ, UK; fax: +44 1223 336033.

CCDC 2245700 contains the supplementary crystallographic data for this paper. These data can be obtained free of charge via www.ccdc.cam.ac.uk/data_request/cif, or by emailing data_request@ccdc.cam.ac.uk, or by contacting The Cambridge Crystallographic Data Centre, 12 Union Road, Cambridge CB2 1EZ, UK; fax: +441,223 336,033.

Complete contact information is available at: https://pubs.acs.org/10.1021/jacs.3c02273

The authors declare no competing financial interest.

Abstract

Lytic polysaccharide monooxygenases have received significant attention as catalytic convertors of biomass to biofuel. Recent studies suggest that its peroxygenase activity (i.e., using H_2O_2 as an oxidant) is more important than its monooxygenase functionality. Here, we describe new insights into peroxygenase activity, with a copper(I) complex reacting with H_2O_2 leading to site-specific ligand–substrate C–H hydroxylation. $\left[Cu^{I}(TMG_3tren)\right]^{+}$(**1**) ($TMG_3tren = 1,1,1-Tris\left\{2-[N^2-(1,1,3,3-tetramethylguanidino)]ethyl\right\}amine$) and a dry source of hydrogen peroxide, $(o-Tol_3P=O\cdot H_2O_2)_2$ react in the stoichiometry, $\left[Cu^{I}(TMG_3tren)\right]^{+}+H_2O_2\rightarrow\left[Cu^{I}(TMG_3tren\text{-}OH)\right]^{+}+H_2O$, wherein a ligand *N*-methyl group undergoes hydroxylation giving TMG_3tren-OH. Furthermore, Fenton-type chemistry ($Cu^{I}+H_2O_2\rightarrow Cu^{II}-OH+\cdot OH$) is displayed, in which (i) a $Cu(II)-OH,(\cdot OH)$ complex could be detected during the reaction and it could be separately isolated and characterized crystallographically and (ii) hydroxyl radical (·OH) scavengers either quenched the ligand hydroxylation reaction and/or (iii) captured the ·OH produced.

Graphical Abstract

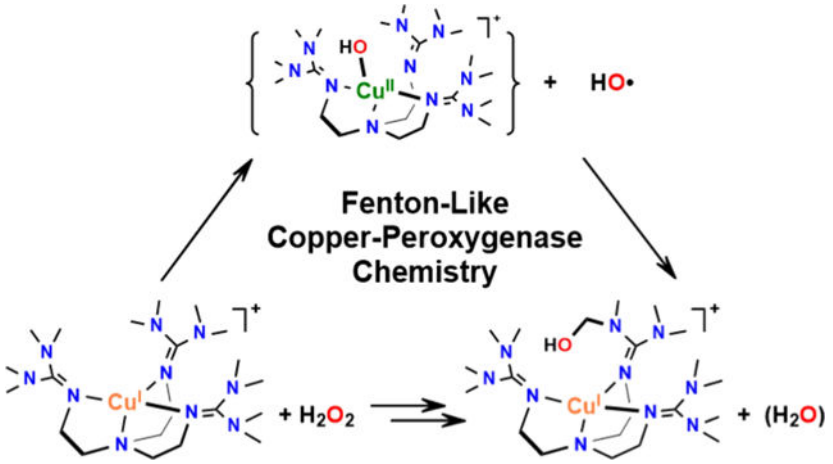

INTRODUCTION

Oxidative degradation of biomass such as chitin and cellulose is known[1] to be carried out by bacterial and fungal lytic polysaccharide monooxygenases (LPMOs) which comprise a component of the carbohydrate active enzymes (CAZy) family.[2,3] These mononuclear copper enzymes enable active-site chemistry in the oxidation of recalcitrant polysaccharide C1 and/or C4 C–H bonds (see the diagram in the SI[4]) possessing bond dissociation energies of ~101−104 kcal/mol.[5] Thus, there is considerable potential to generate biofuels in a sustainable manner, by utilizing LPMOs to break down plentiful biomass materials.[1c,2c]

Earlier studies revealed a classical monooxygenase activity for LPMOs (Scheme 1a)[1c,2a,6] which possess a mononuclear Cu active site with a tridentate T-shaped coordination, having protein-derived ligation from 2 His residue imidazole N's plus a primary amine

($-NH_2$) derived from the N-terminal His; the latter comprises a chelate, referred to as the "His brace".[1b,3b,7] In a monooxygenase reaction cycle,[8] a cupric-superoxide $\left(Cu^{II}(O_2^{\cdot -})\right)$ species could form via initial O_2-interaction with a copper(I) center.[2b,8b,9] This could directly do HAA or, following electron and/or proton transfers would lead to a Cu^{II}-(hydro)peroxide entity that is further transformed into the key species which would affect the difficult hydrogen-atom abstraction (HAA) reaction (e.g., a copper(II)-oxyl $\left(Cu^{II}-O\cdot\right)$ species).[1d,3a,8b,10]

However, in fact, recent biochemical−biophysical studies[10i,11] detail that LPMOs also are widely functional as peroxygenases and that H_2O_2 is faster reacting with reduced copper(I) LPMOs than is molecular oxygen. The peroxygenase biochemistry (Scheme 1b) is found to lead to observable protein damage resulting in lower product yields and loss of reaction selectivity in comparison to the O_2-mediated monooxygenase reactivity. Also, computational studies support the viability of LPMO peroxygenase activity.[10h,12] Scheme 1c provides mechanistic pathways which have been proposed or can be considered, for the enzyme ligand−copper(I) ion/H_2O_2 chemistry leading to substrate hydroxylation. The likely reactive species capable of HAA for these difficult substrates are (i) a hydroxyl radical (·OH) produced by copper Fenton chemistry, $\left(Cu^{I}+H_2O_2\rightarrow Cu^{II}-OH+\cdot OH\right)$ (and see below),[13] (ii) a $Cu^{II}-O\cdot\cdot$ species which may be directly generated from a $Cu^{I}+H_2O_2$ reaction with release of H_2O_2; a related route, that has been suggested, could be if the ·OH moiety produced in the Fenton-like reaction, abstracts an H-atom from the Cu^{II}-hydroxide moiety, $Cu^{II}-OH+\cdot OH\rightarrow Cu^{II}-O\cdot+H_2O$ (Scheme 1c)[8b,12,14] and (iii) a high-valent Cu(III) species,[15] possibly a $Cu^{III}(OH)_2$ complex (not shown in Scheme 1) derived from direct homolytic cleavage of H_2O_2 in its interaction with Cu^{I}. The reactive species $Cu^{III}(OH)_2$ would affect substrate C−H bond HAA, with one hydroxide bound to copper accepting the proton and then producing H_2O, leaving behind a Cu^{II}-hydroxide species and the substrate carbon radical (R·); rebound,[16] $Cu^{II}-OH+R\cdot\rightarrow Cu^{I}+R-OH$, would complete a catalytic cycle.

Several recent biochemical studies[10i,17] on the Cu^{I}/H_2O_2 enzyme reaction reveal generation of protein radicals, via one-electron oxidation of a Tyr and Trp residue near the active site. Solomon and co-workers[10i] could demonstrate direct Cu^{II} hydroxide formation concomitant with protein radical formation, potentially derived from the ·OH generated and subsequent reactivity. These observations suggest that scenarios (i) or (ii) (see above) may apply, wherein a copper-mediated Fenton reaction initially occurs in LPMOs. Supporting computational results have been published.[10h,12]

In the Fenton reaction (with Fe^{II} or Cu^{I}),[13a–c,18] the particular situation present (e.g., pH in aqueous media, ligand identity) dictates whether ·OH or a high-valent metal-oxo complex forms (e.g., $Fe^{IV}=O$);[19] under physiological conditions, carbonate radical anion ($CO_3\cdot^-$) is present, rather than ·OH.[13a–c] It is well known that iron- or copper ion-mediated Fenton chemistry effect biological substrate metal-ion/H_2O_2 oxidative damage to peptides or nucleic

acids, where ·OH may be generated and react in a site-specific (or localized) manner,[20] including possibly in LPMOs.[12] Hydrogen peroxide (or −OOH) can reduce copper(II) complexes,[10d,21,22] yielding cuprous ions left to react with any excess H_2O_2 present, leading to Fenton chemistry. Furthermore, a recent report indicates conditions where H_2O_2 reduction of copper(II) coordination complexes is observed; this can occur in situations where the ligand which is binding to the metal ion strongly favors copper(I) (e.g., 2,9-dimethyl-1,10-phenanthroline vs 1,10-phenanthroline), and ·OH is formed if water is present.[23]

More broadly, it has been recently suggested that nature may control metal-ion active site oxidative chemistries by utilizing the Fenton reaction in a "constructive manner".[24] It should also be noted that the hydroxyl radical may be generated by photolysis of water at metal/alloy surfaces (or even at the water−gas surface of water microdroplet)[25] and in a controlled manner be utilized for organic oxidations including conversion of methane to methanol,[26] removal of contaminants in water purification,[27] and chemistry applied to bleaching;[28] it may even be applied to cancer therapies.[29]

Here, we illuminate details concerning a chemical system involving a copper-coordination complex, where an LPMO-type peroxygenase reaction is found to occur. Complex $\left[Cu^{I}(TMG_3tren)\right]^{+}$(**1**) reacts with "dry" H_2O_2,[30] according to Scheme 2, where stoichiometric hydroxylation (i.e., formal insertion of an 'O'-atom) of one of the twelve (12) outer ligand methyl groups occurs:

$$\left[Cu^{I}(TMG_3tren)\right]^{+} + H_2O_2 \rightarrow \left[Cu^{I}(TMG_3tren\text{-}OH)\right]^{+} + H_2O$$

This is a peroxygenase reaction; as Cu^{I} is left as a final product, a potentially catalytic system is established. As described in this report, our conclusion is that this peroxygenase reaction proceeds via Fenton-type chemistry with copper. Among the experimental observations supporting our supposition, are that a Cu^{II}-hydroxide intermediate could be detected (see below) and that an ·OH reactive species (or an equivalent) could be quenched and/or captured.

RESULTS AND DISCUSSION

$\left[Cu^{I}(TMG_3tren)\right]^{+}$(**1**) (Scheme 2) possesses a tripodal tetradentate N_4 ligand with strong (highly basic) alkylamine donor groups, thus having some similarity to the nitrogenous ligand environment found at the LPMO Cu-active sites. Complex **1** is known to reversibly bind molecular oxygen giving $\left[Cu^{II}(TMG_3tren)(O_2^{\cdot -})\right]^{+}$,[31] and it was previously observed that under specific oxidizing conditions, an alkoxide−copper(II) complex $\left[Cu^{II}(TMG_3trenO^{-})\right]^{+}$(**2**) could be isolated and structurally (X-ray) characterized (Figure 1a);[32] this observation suggested that a ligand methyl group had undergone hydroxylation.

The experimental observations in that study led to our suggestions that the most likely reactive species which effected the ligand hydroxylation was a Cu^{II}-hydroperoxide, generated (i) directly from $\left[Cu^{II}(TMG_3tren)\right]^{2+} + H_2O_2(aq) + base$, or (ii) by 1-hydroxy-2,2,6,6-tetramethyl-piperidine (TEMPO-H) reductive protonation of the superoxide complex $\left[Cu^{II}(TMG_3tren)(O_2^{\cdot -})\right]^{+}$, or (iii) by reduction of $\left[Cu^{II}(TMG_3tren)\right]^{2+}$ and/or $\left[Cu^{II}(TMG_3tren)(O_2^{\cdot -})\right]^{+}$ effected by phenols which were added. We also speculated that a $Cu^{II}(-OOH)$ could undergo O–O cleavage leading to product, via a $Cu^{II}-O\cdot$ species, since the reaction of (1) with PhIO also yielded the hydroxylated ligand alkoxide $\left[Cu^{II}(TMG_3trenO^{-})\right]^{+}$. However, as discussed and referenced above (Introduction), ligand-copper(II) complexes can be reduced with hydrogen peroxide, and we have ourselves observed such reactivity which appeared to lead to Cu^{I}/H_2O_2 Fenton chemistry.[10d] Could reduction of copper(II) to copper(I) in the presence of hydrogen peroxide be involved in that 2008 study?

Thus, we thought to take advantage of this chemical system and explore new chemistry with **1** where we employ Fenton chemistry conditions that might relate to the peroxygenase chemistry in LPMOs, as described in the Introduction. Would addition of hydrogen peroxide to the cuprous complex lead to ligand methyl group hydroxylation and if so, could mechanistic aspects be investigated?

Here, in testing Cu^{I}/H_2O_2 reactivity, the alkoxide-copper(II) complex **2** was indeed formed in the reaction of **1** with three equiv dry H_2O_2 (via use of 1.5 equiv $(o-Tol_3P=O\cdot H_2O_2)_2$)[33] in 2-methyltetrahydrofuran (MeTHF) at −70 °C (Scheme 3). A dry solid material source of H_2O_2 allows for careful stoichometric additions as well as use of organic solvents and cryogenic reaction conditions. Observed in the **1**/H_2O_2 reaction was a change from colorless to the green compound **2** $\left\{\lambda_{max}\left(\epsilon, M^{-1}cm^{-1}\right): 420(500),\ 875(270)nm\right\}$ (Figure 1b). A frozen solution EPR spectrum of the reaction solution (Figure 1c) showed, as previously observed, for $\left[Cu^{II}(TMG_3trenO^{-})\right]^{+}$(**2**),[34] a reverse axial signal typical of Cu(II) in a trigonal bipyramidal environment. As was determined previously using ESI-MS,[32] we here also confirmed the formation of alkoxide complex $\left[Cu^{II}(TMG_3trenO^{-})\right]^{+}$(**2**) employing cold spray ionization mass spectrometry (CSI-MS); **2** is characterized by a peak at m/z 5 18 . 3 (calcd m/z 5 18 . 3; Figure 1d).

Time resolution of the reaction was achieved by quickly injecting $(o-Tol_3PO\cdot H_2O_2)_2$ into a −70 °C solution of **1** into the prechilled CSI-MS instrument.[4] The mass spectra clearly show peaks due to $\left[Cu^{II}(TMG_3tren)(OH)\right]^{+}$ ($m/z = 520.3$) at 10 and 54 s. This diminishes as an increasing amount of $\left[Cu^{II}(TMG_3trenO^{-})\right]^{+}$ ($m/z = 518.3$) forms; the final product alkoxide builds up as the Cu^{II}-hydroxide intermediate disappears. Since we have not quantitatively determined instrument response factors for the hydroxide vs alkoxide complexes, strictly speaking we can only say that the hydroxide complex (**3**) forms first. At 120 s, the CSI-MS

signal is essentially pure Cu^{II}-alkoxide **2**; the m/z 520 peak is exactly the intensity expected and observed for authentic **2**,[4] possessing a normal isotope distribution pattern (the effect of $^{63}Cu/^{65}Cu$ isotope abundance). In fact, we show stronger and clearer evidence for initial formation of $\left[Cu^{II}(TMG_3tren) - (OH)\right]^+$ (**3**) in other experiments, see below.

At this stage of experiments, the above results suggest:

$$\left[Cu^{I}(TMG_3tren)\right]^+(\mathbf{1}) + H_2O_2 \rightarrow \left[Cu^{II}(TMG_3tren)(OH)\right]^+(\mathbf{3}) + \cdot OH \quad (1)$$

one of the reaction sequences described above and indicated in Scheme 1, essentially the classical Fenton reaction (with copper(I)). Independently, we could generate copper(II) −hydroxo complex $\left[Cu^{II}(TMG_3tren)(OH)\right]^+(\mathbf{3})$[4] and characterize experimentally its structure via single-crystal X-ray crystallography (Figure 2).[4] Unlike the alkoxide complex $\left[Cu^{II}(TMG_3trenO^-)\right]^+(\mathbf{2})$, no prominent charge-transfer band is apparent for **3**;[4] however, it does display a reverse-axial EPR spectrum ($g_\perp = 2.22$ ($A_\perp = 70$ G) and $g_\parallel = 1.99$ ($A_\parallel = 85$ G)) and a prominent parent ion peak at m/z of 520.3 in CSI-MS.[4]

If the reaction in eq 1 occurs, or even if the products of $\mathbf{1} + H_2O_2$ are $\left(Cu^{II} - O\cdot + H_2O\right)$ or $Cu^{III}(OH)_2$ (see above), the ·OH (formally) would attack one of the ligand methyl groups in order to proceed to the alkoxide product, **2**. We now present experiments whose results suggest that this is likely the case. When excess $\left[Cu^{I}(TMG_3tren)\right]^+(\mathbf{1})$ is reacted with the H_2O_2 reagent, $\left[Cu^{I}(TMG_3tren)\right]^+(\mathbf{1})/H_2O_2 = 5:1$ (via use of 0.1 equiv $(o - Tol_3P{=}O\cdot H_2O_2)_2$), we see from Figure 3a that these reaction conditions do not lead to the observation of the 420 nm UV − vis band associated with alkoxide $\left[Cu^{II}(TMG_3trenO^-)\right]^+(\mathbf{2})$ (i.e., that shown in Figure 1b). This reaction of excess **1** with H_2O_2, conditions such that only one (1) equiv H_2O_2 would react with one molecule of **1**, reveals that essentially no Cu(II) is produced; we observe only ~5% of expected EPR signal intensity which would be due to the presence of a full equivalent of Cu(II) complex (Figure 3b).[35]

Thus, these results, for reaction conditions where $\left[Cu^{I}(TMG_3tren)\right]^+(\mathbf{1})/H_2O_2 = 5:1$, reveal that:

$$\mathbf{5}\left[Cu^{I}(TMG_3tren)\right]^+ + \mathbf{1}\,H_2O_2 \rightarrow \mathbf{4}\left[Cu^{I}(TMG_3tren)\right]^+ + \mathbf{1}\left[Cu^{I}(TMG_3tren - OH)\right]^+ (+\mathbf{1}\,H_2O)$$

i.e., the oxygenation (by H_2O_2) of the Cu^{I}-bound TMG_3tren ligand in $\left[Cu^{I}(TMG_3tren)\right]^+(\mathbf{1})$, to give hydroxylated ligand TMG_3tren-OH as a copper(I) complex (following rebound; see also, below), occurs via a peroxygenase stoichiometry, the reaction described in Scheme 2.

However, to further confirm these conclusions, it is required that we show that ligand hydroxylation has occurred, i.e., $\left[Cu^{I}(TMG_3tren\text{-}OH)\right]^{+}$ is a product. This is, in fact, the case. For the $\left[Cu^{I}(TMG_3tren)\right]^{+}$(**1**)/$H_2O_2$ = 5:1 reaction, the product mixture was quenched at −70 °C with 2,6-dimethyl phenyl isocyanide (DIMPI, as a strong copper(I) specific ligand), the solvent was removed, and the reaction mixture was warmed to RT and then extracted with KCN/CD_3NO_2.[4] MALDI-TOF MS analysis shows that the most intense peak present is due to unreacted ligand TMG_3tren (Figure 3c: m/z 441.3, $\left\{(TMG_3tren) + H^{+}\right\}$ (calcd m/z 441.3)) which was present in excess. The other major product is one where the methyl group of one ligand has been converted to a $-CH_2OH$ (TMG_3tren-OH) functionality and in amounts closely correlating with the quantity of H_2O_2 added, m/z 479.2, $\left\{(TMG_3tren\text{-}OH) + Na^{+}\right\}$ (calcd m/z 479.3; Figure 3c). The TMG_3tren-OH peak has very close to 1/4 of the intensity as the peak due to unhydroxylated ligand, TMG_3tren. Thus the reaction yields are very high, appearing to be nearly quantitative since with the limited amount of H_2O_2 present, only one out of 5 mole-equiv of $\left[Cu^{I}(TMG_3tren)\right]^{+}$(**1**) can undergo conversion to TMG_3tren-OH.

Additional CSI-MS based experiments with these reaction conditions where $\left[Cu^{I}(TMG_3tren)\right]^{+}$(**1**)/$H_2O_2$ = 5:1 provide very strong evidence for the Scheme 2 sequence of reactions, i.e., that $\left[Cu^{II}(TMG_3tren)(OH)\right]^{+}$(**3**) is the initially formed species (as an intermediate). By contrast to the reaction conditions with excess hydrogen peroxide, i.e., the data shown in Figure 1, here $\left[Cu^{II}(TMG_3tren)(OH)\right]^{+}$(**3**) ($m/z$ = 520.3) is formed in a highly persistent manner (Figure 3d), lasting for many minutes prior to the start to observing alkoxide $\left[Cu^{II}(TMG_3trenO^{-})\right]^{+}$(**2**) formation ($m/z$ = 518.3; Figure 3d, from 7 min after sample injection, on). It should be emphasized that formation of hydroxide complex **3** implies that the hydroxyl radical must be forming concomitantly (also see Scheme 2).

Experimental observations that further support our characterization of this peroxygenase system (Scheme 2) are:

1. The TMG_3tren ligand has been hydroxylated prior to formation of the final Cu^{II}-alkoxide complex, supporting the reaction as given by eq 1 (vide supra). When the $\left[Cu^{I}(TMG_3tren)\right]^{+}$(**1**)/$H_2O_2$ = 1:3 is quenched prior to alkoxide $\left[Cu^{II}(TMG_3trenO^{-})\right]^{+}$(**2**) formation (based on following UV−vis changes up to where the 420 nm absorption just starts to be observable), a similar workup and analysis of organics reveal that high yields (>95%) of TMG_3tren-OH are obtained. The prominent ion peak at m/z of 457.2 is assigned to $\left\{(TMG_3tren\text{-}OH) + H^{+}\right\}$ (calcd m/z 457.3; Figure 4a). Only a trace peak for the starting initial unhydroxylated ligand, TMG_3tren (m/z 441.3), is observed in the MALDI-TOF MS spectrum (Figure 4a).

2. With the excess dry H_2O_2 added, we observed additional products of ligand oxygenation, including the overoxidized aldehyde product. Following workup of the reaction mixture containing $\left[Cu^{II}(TMG_3trenO^-)\right]^+$(**2**) and utilizing the DIMPI procedure to remove copper ions (vide supra), mass spectrometric analysis of the organics present reveals that together with a small amount of un-oxidized/oxygenated TMG_3tren, several ligand oxidized types are present (Figure 4). They are (i) the ligand hydroxylated alcohol **L-OH** $\left\{[TMG_3tren-(CH_3)N-CH_2OH]+Na^+\right\}$ (m/z 479.2, calcd m/z 479.3; Figure 4b), (ii) the N–H species arising from TMG_3tren-$(CH_3)N-CH_2OH$ *N*-dealkylation, **L-NH**, $\left\{[TMG_3tren-(CH_3)N-H]+K^+\right\}$ (m/z 465.2, calcd m/z 465.3; Figure 4b), (released formaldehyde is observed),[4] and (iii) a small amount of overoxidized aldehyde species **L-CHO** $\left\{[TMG_3tren$-$(CH_3)N-C(O)H]+K^+\right\}$ (m/z 493.2, calcd m/z 493.3; Figure 4b).

To provide still further evidence for this Fenton-like chemistry, we sought to identify the presence of ·OH (or its equivalent) by employing trapping reagents and/or external substrates which have C–H/O – H bonds (Scheme 4). Inclusion of ten (10) equiv 2,4,6-tri-*t*-butylphenoxyl radical (T*t*BuArO·) with solutions of $\left[Cu^{I}(TMG_3tren)\right]^+$(**1**) prior to addition of H_2O_2(**1**/H_2O_2 = 5:1) quells the peroxygenase type ligand hydroxylation chemistry (Scheme 2); little or no alkoxide complex **2** is formed (UV−vis criterion). We deduce that ·OH produced by the **1**/H_2O_2 reaction reacts with excess T*t*BuArO· present, and elimination of isobutylene (formed in 59% yield) as well as additional documented phenolic chemistry[36] gives 2,6,-di-*t*-butyl-1,4-hydroquinone (as explained in the SI), which is detected in GC−MS as 2,6-di*tert*-butyl-1,4-benzoquinone formed in 20% yield based on copper (so effectively ~100%).[4] This implies capture of "·OH" in near quantitative yields. However, addition of only two equiv. T*t*BuArO· gave only an ~25% yield of the benzoquinone; the efficiency of trapping goes up as the quantity of added trapping agent is increased. Related experiments with excess H_2O_2 and monitored by EPR spectroscopy are also consistent with our conclusions (Figure S5).[4]

For an experiment where 10 equiv trityl radical were added (as Gomberg's dimer) (Scheme 4), again no alkoxide complex **2** formed (UV−vis criterion). Here, the ·OH released from the copper complex (**1**)/H_2O_2 reaction would be trapped by the trityl radical to directly form triphenylcarbinol; this was generated in 18% yield. As was mentioned above, due to the stoichiometry of this reaction, this 18% yield is very high, as 20% is the theoretical maximum. Again, when only a limited amount of added Gomberg's dimer is used (2 equiv), the trapping efficiency is only 3% based on the amount of copper and the stoichiometry of reaction employed (**1**/H_2O_2 = 5:1). Excess amounts of added 2,6-di-*t*-butyl-4-methoxyphenol or xanthene were also observed to "capture" the ·OH generated in reactions of **1** with H_2O_2 (Scheme 4), through HAA to produce 2,6-di-*t*-butyl-4-methoxy phenoxyl radical and xanthone, respectively.[4] See Table S3 for details/yields for the trapping/quenching experiments.

It is interesting to survey a number of recently published LPMO biomimetic studies.[22,37] In those reports involving ligand−copper(II) complex reactions with added hydrogen peroxide and an oxidizable substrate, Simaan and Hitomi,[37a] Kaizer,[22] Itoh,[37b] Castillo,[37c,d] Cowan,[37e] and their co-workers have utilized mono- or poly-nuclear Cu^{II}-complexes, some with a His-Brace like ligand. Added H_2O_2 (aq) likely leads to Cu^{II}-OOH moiety and to oxidation of ligands (e.g., ACC oxidase substrate analogs) or exogenous glucose derivatives (e.g., as polysaccharides or surrogates). However, neither a specific O_2 reduced-derivative (e.g., ·OH) nor a metal-based strong oxidant (e.g., a Cu^{II}-oxyl) has been yet identified. It is notable, however, that Simaan and Hitomi,[37a] and Kaizer[22] provide evidence that excess H_2O_2 at some stage effects cupric ion reduction (via Cu−O heterolytic cleavage of the presumed Cu^{II} – OOH moiety)[10c,10,21b] and the real oxidant species is something like "Cu^{I} – OOH." This latter hypothesis points to Fenton-like reactivity.

Based on these experimental results, we can establish plausible reaction pathways for the $\left[Cu^{I}(TMG_3tren)\right]^{+}$(**1**) and dry H_2O_2 reaction which leads to C−H activation in an overall peroxygenase reaction, shown in Scheme 5 for the differing stoichiometries tested experimentally. The most likely initial reaction is formation of a Cu^{II}-hydroxide complex (**3**) plus a ·OH species. The latter reactive entity performs HAA from a ligand methyl group, producing water and a ligand carbon radical; subsequent rebound from the Cu^{II}-hydroxide gives $Cu^{I}(TMG_3tren\text{-}OH)$.[38] This reaction mechanism was evaluated and is further supported, by density functional theory (DFT) calculations on the full complex and its reaction with H_2O_2.

Figure 5 shows the calculated reaction coordinate based on the proposed mechanism in Scheme 5, top (see the SI for computational details). In the initial structure (Figure 5, **0**), the H_2O_2 associates with the complex through van der Waals interactions but does not bind directly to the Cu (Cu−O distance: 3.27 Å). The reaction proceeds through homolytic cleavage of the H_2O_2 forming a Cu^{II} – OH and ·OH that is 14.9 kcal/mol downhill in ΔG (Figure 5, **2**) through a low barrier of $\Delta G^{\ddagger} = 3.0$ kcal/mol (Figure 5, **1**). Immediately after homolytic cleavage, the resulting ·OH (Figure 5, **2a**) is not properly oriented to abstract an H atom from the ligand methyl group and must reorient to the proper conformation (Figure 5, **2b**) to perform HAA from the C−H bond. This rearrangement involves a small increase in the O···O distance (2.25 Å in **2a** to 2.56 Å in **2b**) and a rotation of the ·OH fragment; this proceeds through a low barrier of 0.9 kcal/mol (Figure 5, **2a**–**2b**). From **2b**, the ·OH performs HAA from the ligand methyl C−H bond with almost no barrier, $\Delta G^{\ddagger} = 0.35$kcal/mol (Figure 5, **3**), producing a water molecule and the ligand methyl radical. This HAA step is further downhill by 23.1 kcal/ mol in ΔG (Figure 5, **4**). Finally, the methyl radical rebound occurs with the highest barrier in this process, $\Delta G^{\dagger} = 7.0$kcal/mol (Figure 5, **5**), due to the significant steric reorganization of the complex to reach this transition state. The Cu^{I} hydroxylated ligand complex product **6** (i.e., $Cu^{I}(TMG_3tren\text{-}OH)$) is 28.1 kcal/mol downhill from the previous step and 66.5 kcal/mol downhill from the starting structure. Each step in the proposed mechanism is thermodynamically favorable, with very low barriers for

O–O cleavage and HAA, and a reasonable, limiting barrier for the rebound hydroxylation. Furthermore, the ·OH reorientation to a conformation conducive to HAA from the ligand would result in a finite lifetime for the $Cu^{II}-OH$ and ·OH, consistent with the observation of species **3** by ESI-MS (Figures 2 and 3) and the radical trapping results. Thus, the calculations in Figure 5 show that the proposed mechanism in Scheme 5 is thermodynamically and kinetically feasible, and consistent with the experimental results presented above.

Scheme 2 and the upper part of Scheme 5 represent a first round of a peroxygenase catalytic cycle, as Cu(I) is regenerated and can accept a new substrate (here, a new unhydroxylated ligand). However, when excess H_2O_2 is present (Scheme 5, bottom), $\left[Cu^{I}(TMG_3tren\text{-}OH)\right]^{+}$ is oxidized by hydrogen peroxide to a cupric form, subsequently leading to TMG_3tren-OH deprotonation and formation of alkoxide $\left[Cu^{II}(TMG_3trenO^{-})\right]^{+}$(**2**). *N*-Dealkylation can otherwise occur (vide supra), producing formaldehyde plus a $Cu^{II}(TMG_3tren\text{-}(CH_3)N-H)$ species, as we observe experimentally.

CONCLUSIONS

In this study, we have provided considerable new insights into site-specific Fenton-type peroxygenase chemistry, quite likely relevant to LPMOs[39] and perhaps also to copper-dependent *p*-methane monooxygenases (*p*MMOs).[24,40] Using a synthetic analog $\left[Cu^{I}(TMG_3tren)\right]^{+}$(**1**), Cu^{I}/H_2O_2 reactions occur. Our experimental results indicate that this leads to a cupric-hydroxide plus hydroxyl radical as suggested in the study on a LPMO by Solomon and co-workers;[10i] subsequent *N*-methyl group hydroxylation occurs leaving behind Cu^{I}. The generation of a ·OH intermediate (or possibly a $Cu^{III}(OH)_2$ or $Cu^{II}-O\cdot$ species) was demonstrated via capture or quenching with radical scavengers or external substrates. The proposed reaction mechanism is further determined to be thermodynamically and kinetically feasible by DFT reaction coordinate calculations. The overall reaction, $\left[Cu^{I}(TMG_3tren)\right]^{+} + H_2O_2 \rightarrow \left[Cu^{I}(TMG_3tren\text{-}OH)\right]^{+}$ $(+H_2O)$, is consistent with LPMO peroxygenase catalytic behavior. This study provides a fresh perspective on Fenton-like copper chemistry and previously proposed mechanisms and nature of key intermediates in peroxygenase reactivity, including LPMOs.

Supplementary Material

Refer to Web version on PubMed Central for supplementary material.

ACKNOWLEDGMENTS

This research was supported by the U.S. National Institutes of Health (NIH) under Awards R35GM139536 (K.D.K.) and DK31450 (E.I.S.).

REFERENCES

(1). (a)Vaaje-Kolstad G; Westereng B; Horn SJ; Liu Z; Zhai H; Sorlie M; Eijsink VGH An Oxidative Enzyme Boosting the Enzymatic Conversion of Recalcitrant Polysaccharides. Science 2010,

330, 219–222. [PubMed: 20929773] (b)Quinlan RJ; Sweeney MD; Lo Leggio L; Otten H; Poulsen J-CN; Johansen KS; Krogh KBRM; Jørgensen CI; Tovborg M; Anthonsen A; Tryfona T; Walter CP; Dupree P; Xu F; Davies GJ; Walton PH Insights into the oxidative degradation of cellulose by a copper metalloenzyme that exploits biomass components. Proc. Natl. Acad. Sci. U. S. A 2011, 108, 15079–15084. [PubMed: 21876164] (c)Hemsworth GR; Henrissat B; Davies GJ; Walton PH Discovery and characterization of a new family of lytic polysaccharide monooxygenases. Nat. Chem. Biol 2014, 10, 122–126. [PubMed: 24362702] (d)Wang B; Wang Z; Davies GJ; Walton PH; Rovira C. Activation of O_2 and H_2O_2 by Lytic Polysaccharide Monooxygenases. ACS Catal. 2020, 10, 12760–12769.

(2). (a)Vu VV; Beeson WT; Span EA; Farquhar ER; Marletta MA A family of starch-active polysaccharide monooxygenases. Proc. Natl. Acad. Sci. U. S. A 2014, 111, 13822–13827. [PubMed: 25201969] (b)Hangasky JA; Detomasi TC; Marletta MA Glycosidic Bond Hydroxylation by Polysaccharide Monooxygenases. Trends Chem. 2019, 1, 198–209.(c)Vu VV; Ngo ST Copper active site in polysaccharide monooxygenases. Coord. Chem. Rev 2018, 368, 134–157.

(3). (a)Meier KK; Jones SM; Kaper T; Hansson H; Koetsier MJ; Karkehabadi S; Solomon EI; Sandgren M; Kelemen B. Oxygen Activation by Cu LPMOs in Recalcitrant Carbohydrate Polysaccharide Conversion to Monomer Sugars. Chem. Rev 2018, 118, 2593–2635. [PubMed: 29155571] (b)Ciano L; Davies GJ; Tolman WB; Walton PH Bracing copper for the catalytic oxidation of C−H bonds. Nat. Catal 2018, 1, 571–577.(c)Chylenski P; Bissaro B; Sørlie M; Røhr ÅK; Várnai A; Horn SJ; Eijsink VGH Lytic Polysaccharide Monooxygenases in Enzymatic Processing of Lignocellulosic Biomass. ACS Catal. 2019, 9, 4970–4991.

(4). See Supporting Information.

(5). Hedegård ED; Ryde U. Targeting the reactive intermediate in polysaccharide monooxygenases. J. Biol. Inorg. Chem 2017, 22, 1029–1037. [PubMed: 28698982]

(6). Hangasky JA; Iavarone AT; Marletta MA Reactivity of O_2 versus H_2O_2 with polysaccharide monooxygenases. Proc. Natl. Acad. Sci. U. S. A 2018, 115, 4915. [PubMed: 29686097]

(7). Ipsen JØ; Hallas-Møller M; Brander S; Lo Leggio L; Johansen KS Lytic polysaccharide monooxygenases and other histidine-brace copper proteins: structure, oxygen activation and biotechnological applications. Biochem. Soc. Trans 2021, 49, 531–540. [PubMed: 33449071]

(8). (a)Lee JY; Karlin KD Elaboration of copper−oxygen mediated C−H activation chemistry in consideration of future fuel and feedstock generation. Curr. Opin. Chem. Biol 2015, 25, 184–193. [PubMed: 25756327] (b)Davydov R; Herzog AE; Jodts RJ; Karlin KD; Hoffman BM End-On Copper(I) Superoxo and Cu(II) Peroxo and Hydroperoxo Complexes Generated by Cryoreduction/Annealing and Characterized by EPR/ENDOR Spectroscopy. J. Am. Chem. Soc 2022, 144, 377–389. [PubMed: 34981938]

(9). (a)Kjaergaard CH; Qayyum MF; Wong SD; Xu F; Hemsworth GR; Walton DJ; Young NA; Davies GJ; Walton PH; Johansen KS; Hodgson KO; Hedman B; Solomon EI Spectroscopic and computational insight into the activation of O_2 by the mononuclear Cu center in polysaccharide monooxygenases. Proc. Natl. Acad. Sci. U. S. A 2014, 8797–8802. [PubMed: 24889637] (b)Diaz DE; Quist DA; Herzog AE; Schaefer AW; Kipouros I; Bhadra M; Solomon EI; Karlin KD Impact of Intramolecular Hydrogen Bonding on the Reactivity of Cupric Superoxide Complexes with O−H and C−H Substrates. Angew. Chem., Int. Ed. Engl 2019, 58, 17572–17576. [PubMed: 31469942]

(10). (a)Kunishita A; Ishimaru H; Nakashima S; Ogura T; Itoh S. Reactivity of Mononuclear Alkylperoxo Copper(II) Complex. O−O Bond Cleavage and C−H Bond Activation. J. Am. Chem. Soc 2008, 130, 4244–4245. [PubMed: 18335943] (b)Gagnon N; Tolman WB $[CuO]^+$ and $[CuOH]^+$ Complexes: Intermediates in Oxidation Catalysis? Acc. Chem. Res 2015, 48, 2126–2131. [PubMed: 26075312] (c)Kim S; Saracini C; Siegler MA; Drichko N; Karlin KD Coordination Chemistry and Reactivity of a Cupric Hydroperoxide Species Featuring a Proximal H-Bonding Substituent. Inorg. Chem 2012, 51, 12603–12605. [PubMed: 23153187] (d)Kim S; Ginsbach JW; Lee JY; Peterson RL; Liu JJ; Siegler MA; Sarjeant AA; Solomon EI; Karlin KD Amine Oxidative N-Dealkylation via Cupric Hydroperoxide Cu−OOH Homolytic Cleavage Followed by Site-Specific Fenton Chemistry. J. Am. Chem. Soc 2015, 137, 2867–2874. [PubMed: 25706825] (e)Decker A; Clay MD; Solomon EI Spectroscopy and electronic structures

of mono- and binuclear high-valent non-heme iron-oxo systems. J. Inorg. Biochem 2006, 100, 697. [PubMed: 16510189] (f)Rezabal E; Gauss J; Matxain JM; Berger R; Diefenbach M; Holthausen MC Quantum chemical assessment of the binding energy of CuO^+. J. Chem. Phys 2011, 134, No. 064304.(g)Kim S; Ståhlberg J; Sandgren M; Paton RS; Beckham GT Quantum mechanical calculations suggest that lytic polysaccharide monooxygenases use a copper-oxyl, oxygen-rebound mechanism. Proc. Natl. Acad. Sci. U. S. A 2014, 111, 149–154. [PubMed: 24344312] (h)Wang B; Walton PH; Rovira C. Molecular Mechanisms of Oxygen Activation and Hydrogen Peroxide Formation in Lytic Polysaccharide Monooxygenases. ACS Catal. 2019, 9, 4958–4969. [PubMed: 32051771] (i)Jones SM; Transue WJ; Meier KK; Kelemen B; Solomon EI Kinetic analysis of amino acid radicals formed in H_2O_2-driven Cu^I LPMO reoxidation implicates dominant homolytic reactivity. Proc. Natl. Acad. Sci. U. S. A 2020, 117, 11916. [PubMed: 32414932] (j)Srnec M; Navrátil R; Andris E; Jašík; Roithová J. Experimentally Calibrated Analysis of the Electronic Structure of CuO^+: Implications for Reactivity. Angew. Chem., Int. Ed. Engl 2018, 57, 17053–17057. [PubMed: 30427565] (k)Conde A; Vilella L; Balcells D; Díaz-Requejo MM; Lledós A; Pérez PJ Introducing Copper as Catalyst for Oxidative Alkane Dehydrogenation. J. Am. Chem. Soc 2013, 135, 3887–3896. [PubMed: 23409843]

(11). (a)Bissaro B; Røhr ÅK; Müller G; Chylenski P; Skaugen M; Forsberg Z; Horn SJ; Vaaje-Kolstad G; Eijsink VGH Oxidative cleavage of polysaccharides by monocopper enzymes depends on H_2O_2. Nat. Chem. Biol 2017, 13, 1123–1128. [PubMed: 28846668] (b)Bissaro B; Streit B; Isaksen I; Eijsink VGH; Beckham GT; DuBois JL; Røhr ÅK Molecular mechanism of the chitinolytic peroxygenase reaction. Proc. Natl. Acad. Sci. U. S. A 2020, 117, 1504–1513. [PubMed: 31907317] (c)Brander S; Tokin R; Ipsen JO; Jensen PE; HernandezRollan C; Norholm MHH; Lo Leggio L; Dupree P; Johansen KS Scission of Glucosidic Bonds by a Lentinus similis Lytic Polysaccharide Monooxygenases Is Strictly Dependent on H_2O_2 while the Oxidation of Saccharide Products Depends on O_2. ACS Catal. 2021, 11, 13848–13859.(d)Rieder L; Stepnov AA; Sørlie M; Eijsink VGH Fast and Specific Peroxygenase Reactions Catalyzed by Fungal Mono-Copper Enzymes. Biochemistry 2021, 60, 3633–3643. [PubMed: 34738811]

(12). Wang B; Johnston EM; Li P; Shaik S; Davies GJ; Walton PH; Rovira C. QM/MM Studies into the H_2O_2-Dependent Activity of Lytic Polysaccharide Monooxygenases: Evidence for the Formation of a Caged Hydroxyl Radical Intermediate. ACS Catal. 2018, 8, 1346–1351.

(13). (a)Illés E; Mizrahi A; Marks V; Meyerstein D. Carbonate-radical-anions, and not hydroxyl radicals, are the products of the Fenton reaction in neutral solutions containing bicarbonate. Free Radical Biol. Med 2019, 131, 1–6. [PubMed: 30458276] (b)Patra SG; Mizrahi A; Meyerstein D. The Role of Carbonate in Catalytic Oxidations. Acc. Chem. Res 2020, 53, 2189–2200. [PubMed: 32975405] (c)Meyerstein D. Re-examining Fenton and Fenton-like reactions. Nat. Rev. Chem 2021, 5, 595–597. [PubMed: 37118415] (d)Mitra S; Prakash D; Rajabimoghadam K; Wawrzak Z; Prasad P; Wu T; Misra SK; Sharp JS; Garcia-Bosch I; Chakraborty S. De Novo Design of a Self-Assembled Artificial Copper Peptide that Activates and Reduces Peroxide. ACS Catal. 2021, 11, 10267–10278. [PubMed: 36188417] (e)Trammell R; Garcia-Bosch I. Synthetic Copper Complexes as Cu-Dependent Monooxygenase Model Systems and Catalysts for Dioxygen Reduction and Water Oxidation. In Comprehensive Coordination Chemistry III; Constable EC; Parkin G; Que L Jr, Eds.; Elsevier: Oxford, 2021; pp 436–473.

(14). Hirao H; Li F; Que L; Morokuma K. Theoretical Study of the Mechanism of Oxoiron(IV) Formation from H_2O_2 and a Nonheme Iron(II) Complex: O−O Cleavage Involving Proton-Coupled Electron Transfer. Inorg. Chem 2011, 50, 6637–6648. [PubMed: 21678930]

(15). Pham AN; Xing G; Miller CJ; Waite TD Fenton-like copper redox chemistry revisited: Hydrogen peroxide and superoxide mediation of copper-catalyzed oxidant production. J. Catal 2013, 301, 54–64.

(16). (a)Ryle MJ; Hausinger RP Non-heme iron oxygenases. Curr. Opin. Chem. Biol 2002, 6, 193–201. [PubMed: 12039004] (b)Huang X; Groves JT Oxygen Activation and Radical Transformations in Heme Proteins and Metalloporphyrins. Chem. Rev 2018, 118, 2491–2553. [PubMed: 29286645] (c)Galeotti M; Vicens L; Salamone M; Costas M; Bietti M. Resolving Oxygenation Pathways in Manganese-Catalyzed C(sp3) − H Functionalization via Radical and Cationic Intermediates. J. Am. Chem. Soc 2022, 144, 7391–7401. [PubMed: 35417154] (d)Cowley RE; Tian L; Solomon EI Mechanism of O_2 activation and substrate hydroxylation in

noncoupled binuclear copper monooxygenases. Proc. Natl. Acad. Sci. U. S. A 2016, 113, 12035–12040. [PubMed: 27790986] (e)Zaragoza JPT; Yosca TH; Siegler MA; Moënne-Loccoz P; Green MT; Goldberg DP Direct Observation of Oxygen Rebound with an Iron-Hydroxide Complex. J. Am. Chem. Soc 2017, 139, 13640–13643. [PubMed: 28930448] (f)Guo M; Corona T; Ray K; Nam W. Heme and Nonheme High-Valent Iron and Manganese Oxo Cores in Biological and Abiological Oxidation Reactions. ACS Cent. Sci 2019, 5, 13–28. [PubMed: 30693322]

(17). (a)Paradisi A; Johnston EM; Tovborg M; Nicoll CR; Ciano L; Dowle A; McMaster J; Hancock Y; Davies GJ; Walton PH Formation of a Copper(II)−Tyrosyl Complex at the Active Site of Lytic Polysaccharide Monooxygenases Following Oxidation by H_2O_2. J. Am. Chem. Soc 2019, 141, 18585–18599. [PubMed: 31675221] (b)Singh RK; Blossom BM; Russo DA; Singh R; Weihe H; Andersen NH; Tiwari MK; Jensen PE; Felby C; Bjerrum MJ Detection and Characterization of a Novel Copper-Dependent Intermediate in a Lytic Polysaccharide Monooxygenase. Chem. − Eur. J 2020, 26, 454–463. [PubMed: 31603264]

(18). (a)Goldstein S; Meyerstein D; Czapski G. The Fenton Reagents. Free Radical Biol. Med 1993, 15, 435–445. [PubMed: 8225025] (b)Petit AS; Pennifold RCR; Harvey JN Electronic Structure and Formation of Simple Ferryloxo Complexes: Mechanism of the Fenton Reaction. Inorg. Chem 2014, 53, 6473–6481. [PubMed: 24785907]

(19). (a)Pestovsky O; Stoian S; Bominaar EL; Shan X; Munck E; Que L; Bakac A. Aqueous Fe^{IV} = O: Spectroscopic identification and oxo-group exchange. Angew. Chem., Int. Ed. Engl 2005, 44, 6871–6874. [PubMed: 16206322] (b)Bataineh H; Pestovsky O; Bakac A. pH-induced mechanistic changeover from hydroxyl radicals to iron(IV) in the Fenton reaction. Chem. Sci 2012, 3, 1594–1599.

(20). (a)Stadtman ER Oxidation of free amino acids and amino acid residues in proteins by radiolysis and by metal-catalyzed reactions. Annu. Rev. Biochem 1993, 62, 797–821. [PubMed: 8352601] (b)Stadtman ER; Levine RL Free radical-mediated oxidation of free amino acids and amino acid residues in proteins. Amino Acids 2003, 25, 207–218. [PubMed: 14661084] (c)Sayre LM; Perry G; Smith MA Oxidative Stress and Neurotoxicity. Chem. Res. Toxicol 2008, 21, 172–188. [PubMed: 18052107] (d)Zhang S; Trammell R; Cordova A; Siegler MA; Garcia-Bosch I. Cupromoted intramolecular hydroxylation of C−H bonds using directing groups with varying denticity. J. Inorg. Biochem 2021, 223, No. 111557.

(21). (a)Osako T; Nagatomo S; Tachi Y; Kitagawa T; Itoh S. Low-temperature stopped-flow studies on the reactions of copper(II) complexes and H_2O_2: The first detection of a mononuclear copper(II)-peroxo intermediate. Angew. Chem., Int. Ed. Engl 2002, 41, 4325–4328. [PubMed: 12434378] (b)Kunishita A; Kubo M; Ishimaru H; Ogura T; Sugimoto H; Itoh S. H_2O_2-Reactivity of Copper(II) Complexes Supported by Tris[(pyridin-2-yl)methyl]amine Ligands with 6-Phenyl Substituents. Inorg. Chem 2008, 47, 12032–12039. [PubMed: 18998628]

(22). Pap JS; El Bakkali-Tahéri N; Fadel A; Góger S; Bogáth D; Molnár M; Giorgi M; Speier G; Simaan AJ; Kaizer J. Oxidative Degradation of Amino Acids and Aminophosphonic Acids by 2,2′-Bipyridine Complexes of Copper(II). Eur. J. Inorg. Chem 2014, 2014, 2829–2838.

(23). (a)Romo AIB; dos Reis MP; Nascimento OR; Bernhardt PV; Rodríguez-López J; Diógenes ICN Interplay of electronic and geometric structure on Cu phenanthroline, bipyridine and derivative complexes, synthesis, characterization, and reactivity towards oxygen. Coord. Chem. Rev 2023, 477, No. 214943.(b)Levín P; Ruiz MC; Romo AIB; Nascimento OR; Di Virgilio AL; Oliver AG; Ayala AP; Diógenes ICN; León IE; Lemus L. Water-mediated reduction of $[Cu(dmp)_2(CH_3CN)]^{2+}$: implications of the structure of a classical complex on its activity as an anticancer drug. Inorg. Chem. Front 2021, 8, 3238–3252.

(24). Wang B; Zhang X; Fang W; Rovira C; Shaik S. How Do Metalloproteins Tame the Fenton Reaction and Utilize ·OH Radicals in Constructive Manners? Acc. Chem. Res 2022, 55, 2280–2290. [PubMed: 35926175]

(25). (a)Meng Y; Gnanamani E; Zare RN Direct C(sp3) – N Bond Formation between Toluene and Amine in Water Microdroplets. J. Am. Chem. Soc 2022, 144, 19709–19713. [PubMed: 36255242] (b)Meng Y; Gnanamani E; Zare RN Catalyst-Free Decarboxylative Amination of Carboxylic Acids in Water Microdroplets. J. Am. Chem. Soc 2023, 145, 32–36. [PubMed: 36566437]

(26). (a)Fang G; Hu JN; Tian LC; Liang JX; Lin J; Li L; Zhu C; Wang X. Zirconium-oxo Nodes of MOFs with Tunable Electronic Properties Provide Effective ·OH Species for Enhanced Methane Hydroxylation. Angew. Chem., Int. Ed. Engl 2022, 61, No. e202205077.(b)Jiang Y; Li S; Wang S; Zhang Y; Long C; Xie J; Fan X; Zhao W; Xu P; Fan Y; Cui C; Tang Z. Enabling Specific Photocatalytic Methane Oxidation by Controlling Free Radical Type. J. Am. Chem. Soc 2023, 145, 2698–2707. [PubMed: 36649534]

(27). (a)Cheng C; Ren W; Miao F; Chen X; Chen X; Zhang H. Generation of $Fe^{IV} = O$ and its Contribution to Fenton-Like Reactions on a Single-Atom Iron-N−C Catalyst. Angew. Chem., Int. Ed. Engl 2023, 62, No. e202218510.(b)Li J; Pham AN; Dai R; Wang Z; Waite TD Recent advances in Cu-Fenton systems for the treatment of industrial wastewaters: Role of Cu complexes and Cu composites. J. Hazard. Mater 2020, 392, No. 122261.

(28). (a)Lin T-Y; Wu C-H Activation of hydrogen peroxide in copper(II)/amino acid/H_2O_2 systems: effects of pH and copper speciation. J. Catal 2005, 232, 117–126.(b)Yin C; Huang Y; Zhang L; Xu H; Zhong Y; Mao Z. Low-temperature bleaching of cotton fabric using a copper-based catalyst for hydrogen peroxide. Color. Technol 2015, 131, 66–71.

(29). (a)Santini C; Pellei M; Gandin V; Porchia M; Tisato F; Marzano C. Advances in Copper Complexes as Anticancer Agents. Chem. Rev 2013, 114, 815–862. [PubMed: 24102434] (b)Kang Z; Jiang J; Tu Q; Liu S; Zhang Y; Wang DE; Wang J; Yuan MS Dual-Site Chemosensor for Monitoring ·OH-Cysteine Redox in Cells and In Vivo. J. Am. Chem. Soc 2023, 145, 507–515. [PubMed: 36524839] (c)Li S-L; Chu X; Dong H-L; Hou H-Y; Liu Y. Recent advances in augmenting Fenton chemistry of nanoplatforms for enhanced chemodynamic therapy. Coord. Chem. Rev 2023, 479, No. 215004.

(30). A dry solid material source of H_2O_2 allows for careful stoichiometric additions and use of organic solvents and cryogenic reaction conditions.

(31). (a)Bhadra M; Transue WJ; Lim H; Cowley RE; Lee JYC; Siegler MA; Josephs P; Henkel G; Lerch M; Schindler S; Neuba A; Hodgson KO; Hedman B; Solomon EI; Karlin KD A Thioether-Ligated Cupric Superoxide Model with Hydrogen Atom Abstraction Reactivity. J. Am. Chem. Soc 2021, 143, 3707–3713. [PubMed: 33684290] (b)Würtele C; Gaoutchenova E; Harms K; Holthausen MC; Sundermeyer; Schindler S. Crystallographic Characterization of a Synthetic 1:1 End-On Copper Dioxygen Adduct Complex. Angew. Chem., Int. Ed. Engl 2006, 45, 3867–3869. [PubMed: 16671142]

(32). Maiti D; Lee D-H; Gaoutchenova K; Würtele C; Holthausen MC; Sarjeant AAN; Sundermeyer J; Schindler S; Karlin KD Reactions of a Copper(II) Superoxo Complex Lead to C−H and O−H Substrate Oxygenation: Modeling CopperMonooxygenase C−H Hydroxylation. Angew. Chem., Int. Ed. Engl 2008, 47, 82–85. [PubMed: 18022887]

(33). Arp FF; Bhuvanesh N; Blümel J. Hydrogen peroxide adducts of triarylphosphine oxides. Dalton Trans. 2019, 48, 14312–14325. [PubMed: 31475705]

(34). (a)Jiang F; Karlin KD; Peisach J. An Electron Spin Echo Envelope Modulation (ESEEM) Study of Electron-Nuclear Hyperfine and Nuclear Quadrupole Interactions of dz2 Ground State Cu(II) Complexes with Substituted Imidazoles. Inorg. Chem 1993, 32, 2576–2582.(b)Hathaway BJ Copper. In Comprehensive Coordination Chemistry; Wilkinson G, Ed.; Pergamon: New York, 1987; vol 5, pp 533–774.(c)Lucchese B; Humphreys KJ; Lee DH; Incarvito CD; Sommer RD; Rheingold AL; Karlin KD Mono- Bi- and Trinuclear CuII-Cl Contaninig Products Based on the Tris(2-pyridylmethyl)amine Chelate, Derived from Copper(I) Complex Dechlorinations of Chloroform. Inorg. Chem 2004, 43, 5987–5998. [PubMed: 15360248]

(35). The presence of only copper(I), all 5 equiv, is also demonstrated by oxygenation of this reaction mixture; essentially all Cu present is in the reduced Cu(I) form. See SI.

(36). Lee JY; Peterson RL; Ohkubo K; Garcia-Bosch I; Himes RA; Woertink J; Moore CD; Solomon EI; Fukuzumi S; Karlin KD Mechanistic Insights into the Oxidation of Substituted Phenols via Hydrogen Atom Abstraction by a Cupric−Superoxo Complex. J. Am. Chem. Soc 2014, 136, 9925–9937. [PubMed: 24953129]

(37). (a)Ghattas W; Giorgi M; Mekmouche Y; Tanaka T; Rockenbauer A; Reglier M; Hitomi Y; Simaan AJ Identification of a Copper(I) Intermediate in the Conversion of 1-Aminocyclopropane Carboxylic Acid (ACC) into Ethylene by Cu(II) − ACC Complexes and Hydrogen Peroxide.

Inorg. Chem 2008, 47, 4627–4638. [PubMed: 18442237] (b)Fukatsu A; Morimoto Y; Sugimoto H; Itoh S. Modelling a 'histidine brace' motif in mononuclear copper monooxygenases. Chem. Commun 2020, 56, 5123–5126.(c)Neira AC; Martínez-Alanis PR; Aullón G; Flores-Alamo M; Zerón P; Company A; Chen J; Kasper JB; Browne WR; Nordlander E; Castillo I. Oxidative Cleavage of Cellobiose by Lytic Polysaccharide Monooxygenase (LPMO)-Inspired Copper Complexes. ACS Omega 2019, 4, 10729–10740. [PubMed: 31460171] (d)Castillo I; Torres-Flores AP; Abad-Aguilar DF; Berlanga-Vázquez A; Orio M; Martínez-Otero D. Cellulose Depolymerization with LPMO-inspired Cu Complexes. ChemCatChem 2021, 13, 4700–4704.(e)Yu Z; Thompson Z; Behnke SL; Fenk KD; Huang D; Shafaat HS; Cowan JA Metalloglycosidase Mimics: Oxidative Cleavage of Saccharides Promoted by Multinuclear Copper Complexes under Physiological Conditions. Inorg. Chem 2020, 59, 11218–11222. [PubMed: 32799467] (f)Chen K; Zangiabadi M; Zhao Y. Oxidative Cleavage of Glycosidic Bonds by Synthetic Mimics of Lytic Polysaccharide Monooxygenases. Org. Lett 2022, 24, 3426–3430. [PubMed: 35503979] (g)Bouchey CJ; Shopov DY; Gruen AD; Tolman WB Mimicking the Cu Active Site of Lytic Polysaccharide Monooxygenase Using Monoanionic Tridentate N-Donor Ligands. ACS Omega 2022, 7, 35217–35232. [PubMed: 36211076] (h)Hassoon AA; Szorcsik A; Fulop L; Papp ZI; May NV; Gajda T. Peptide-based chemical models for lytic polysaccharide monooxygenases. Dalton Trans. 2022, 51, 17241–17254. [PubMed: 36314721]

(38). Note: we tested directly for the viability of this latter process and the results support our rebound hypothesis. When the hydroxide complex $\left[Cu^{II}(TMG_3tren)(OH)\right]^+$(**3**) is exposed to 10 equiv trityl radical (as Gomberg's dimer) at −70 °C, $\left[Cu^{I}(TMG_3tren)\right]^+$(**1**) was produced in high yields (ESI detection of 1 and depletion of trityl radical occurred (UV-vis monitoring)) and a 67% yield of triphenylmethanol was obtained. See Supporting Information.

(39). Bissaro B; Eijsink VGH Lytic polysaccharide monooxygenases: enzymes for controlled and site-specific Fenton-like chemistry. Essays Biochem. 2023, 67, 575–584. [PubMed: 36734231]

(40). Peng W; Qu X; Shaik S; Wang B. Deciphering the oxygen activation mechanism at the CuC site of particulate methane monooxygenase. Nat. Catal 2021, 4, 266–273.

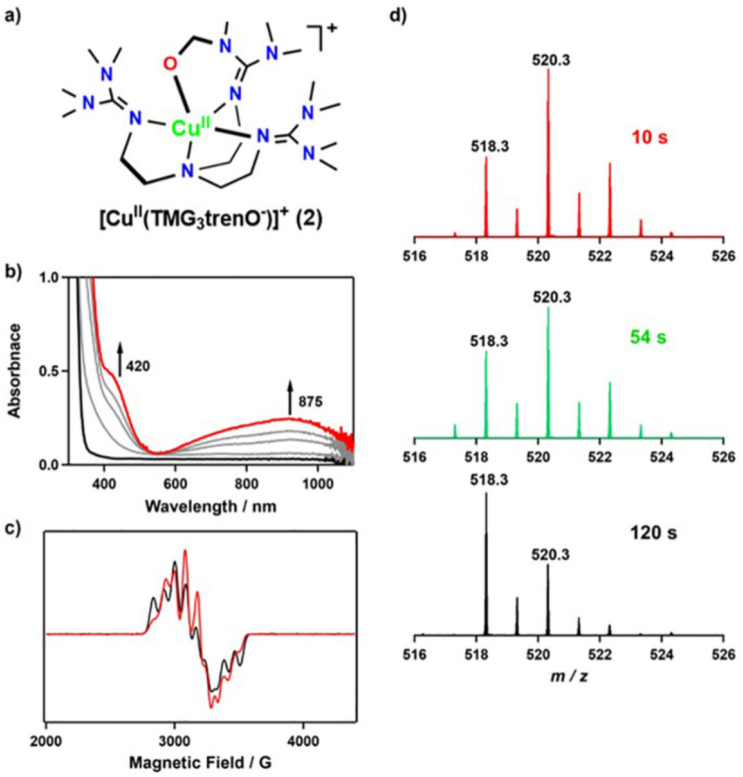

Figure 1.

(a) ChemDraw representation of $\left[Cu^{II}(TMG_3trenO^-)\right]^+$(**2**) based on its crystallographic determination.[32] (b) UV−vis spectral changes (over 1 h) when $\left[Cu^{I}(TMG_3tren)\right]^+$(**1**) reacts with three equiv H_2O_2 in MeTHF at −70 °C. (c) X-band EPR spectrum (red) {$g_\perp = 2.27$ ($A\perp = 82$ G) and $g_\parallel = 1.99$ ($A_\parallel = 82$ G)} and simulation (black) of complex **2** in frozen MeTHF at 20 K. (d) Time-resolution of CSI-MS spectrum for the formation of **2** upon addition of 3 equiv H_2O_2 to a solution of 1 at −70 °C, 10 s (red) after injection, then at 54 s (green), and finally at 120 s (black), which is identified as pure alkoxide complex **2**.

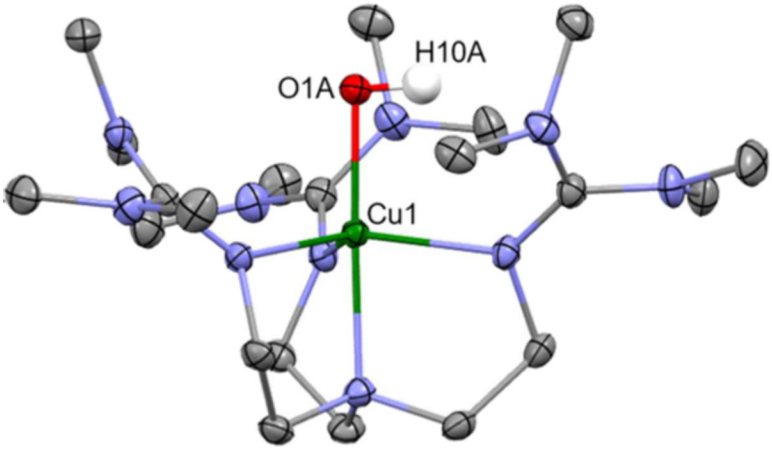

Figure 2.

Displacement ellipsoid plot (30% probability level) of one of the two crystallographically independent $\left[Cu^{II}(TMG_3tren)(OH)\right]^+$ cations (**3**) at 110(2) K. Hydrogen atoms and lattice solvent molecules are omitted for clarity except for a hydrogen atom on the hydroxo ligand. The hydroxo O-atom is H-bonded to two partially occupied crystal lattice water molecules (not shown); O1A···O1W (H-bonding) = 2.771 Å (gray, C; white, H; blue, N; red, O; green, Cu).

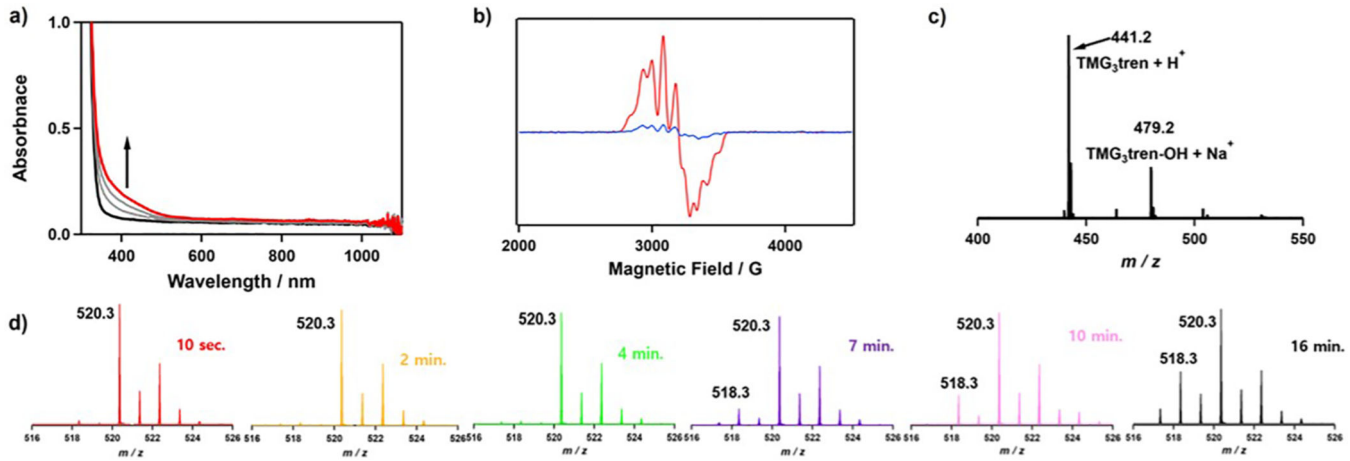

Figure 3.

(a) UV−vis spectral changes of **1** with 0.2 equiv H_2O_2 in MeTHF at −70 °C. (b) X-band EPR spectrum of authentic complex **2** (red) and the product solution obtained with 0.2 equiv H_2O_2 added to **1** (blue) in frozen MeTHF at 20 K. (c) Matrix-assisted laser desorption/ionization-time-of-flight mass spectrometry (MALDI-TOF MS) spectrum; the reaction of excess **1** and H_2O_2 after metal ions were removed by treatment with DIMPI and KCN/CD_3CN. (d) CSI-MS spectra for the reaction of **1** and 0.2 equiv H_2O_2 in MeTHF at −70 °C. The times indicated in the various panels indicate the number of seconds or minutes following sample injection. Also, see the text.

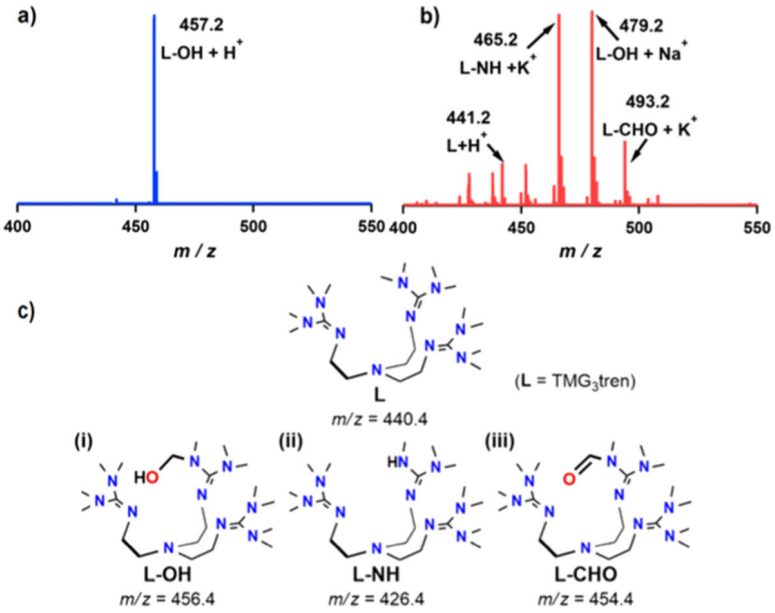

Figure 4.

MALDI-TOF MS spectrum; metal ions removed by treatment with DIMPI and KCN/CD_3CN. (a) Prior to, or (b) after, the formation of Cu^{II}-alkoxide species with excess of H_2O_2 added to **1**. (c) Oxidized products in the reaction of **1** and excess of H_2O_2.

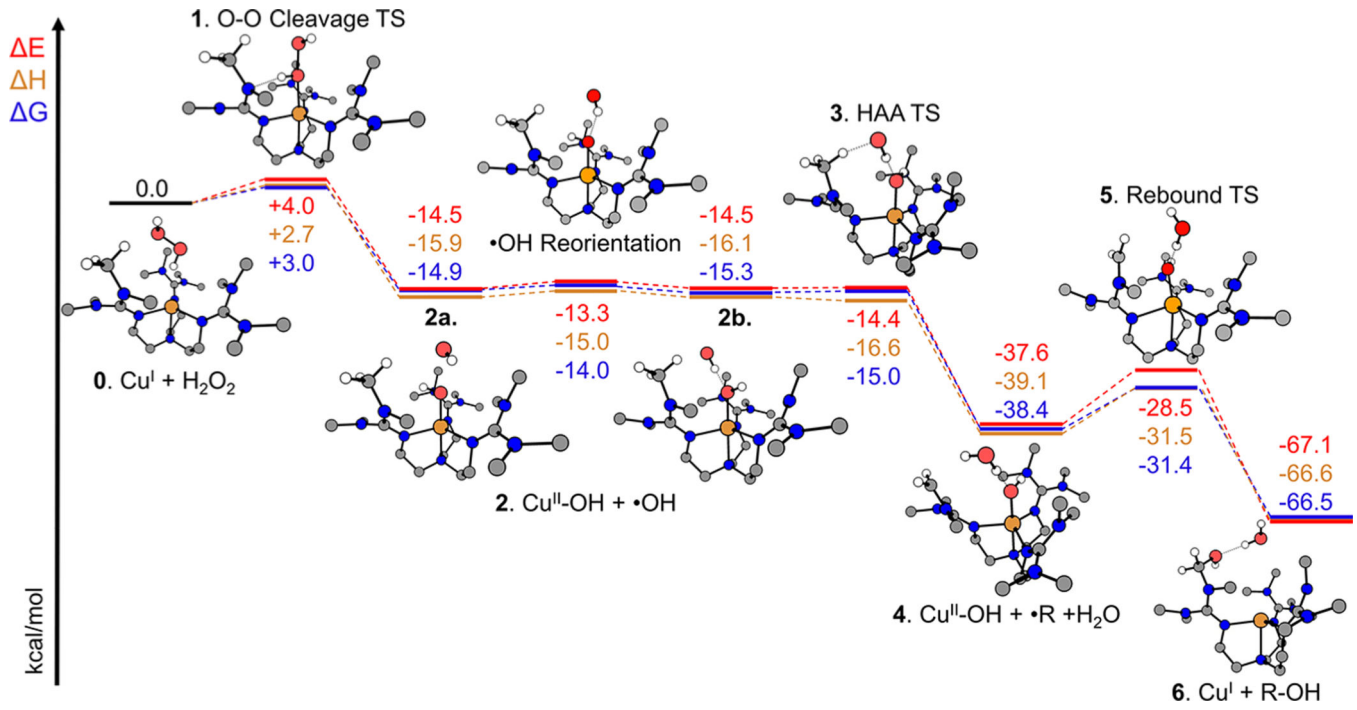

Figure 5.

DFT-calculated reaction coordinate for homolytic H_2O_2 cleavage, subsequent HAA and rebound ligand hydroxylation by $\left[Cu^{I}(TMG_3tren)\right]^{+}$. Optimized structures and singlet energies are shown for each species. Thermodynamics are calculated at −70 °C.

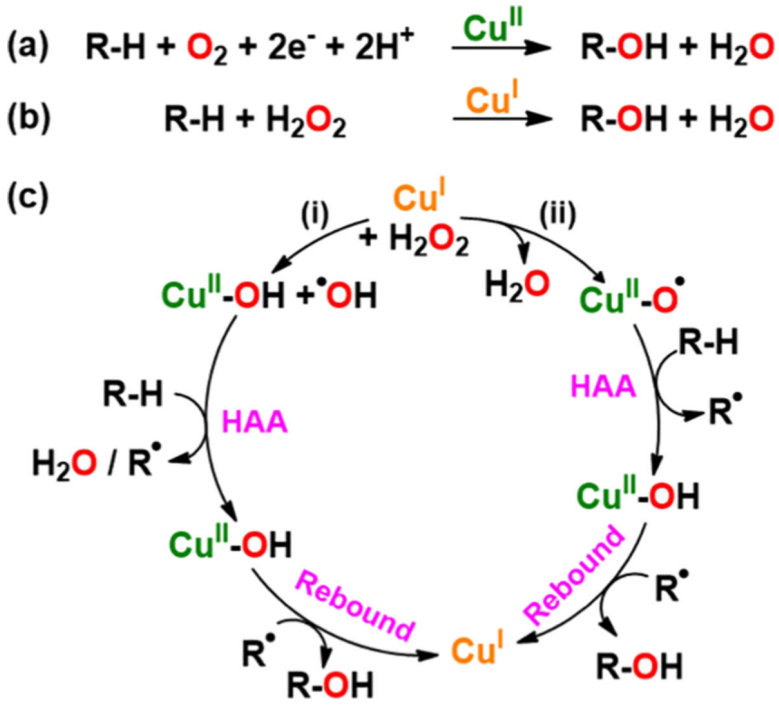

Scheme 1.

LPMO Reaction Scheme (a) Monooxygenase and (b) Peroxygenase Reaction Pathway; (c) Proposed Mechanisms Relevant to the LPMOs Cu-Site, Processing H_2O_2

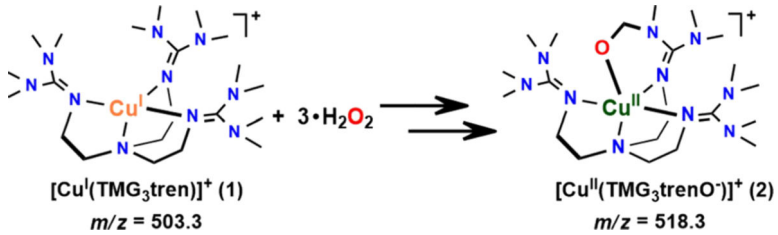

Scheme 3.

Reaction of Complex $\left[Cu^{I}(TMG_3tren)\right]^{+}$(**1**) with 3 equiv H_2O_2 Leads to Cu^{II}-Alkoxide Complex (2)

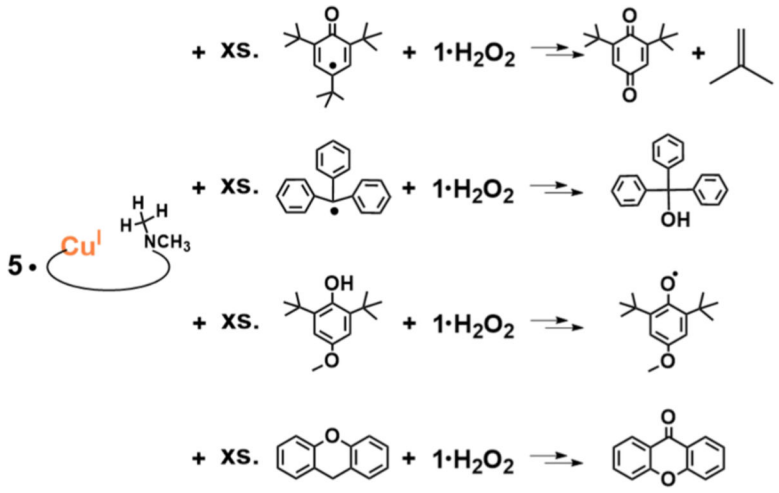

Scheme 4.

Capture/Trapping of a Hydroxyl Radical (·OH) Derived from $\left[Cu^{I}(TMG_3tren)\right]^{+}$(**1**) Reactivity with Hydrogen Peroxide[a]

[a] Partial or nearly full inhibition of the peroxygenase chemistry where **1** is converted to alkoxide $\left[Cu^{II}(TMG_3trenO^{-})\right]^{+}$(**2**) occurs. Also, see the text.

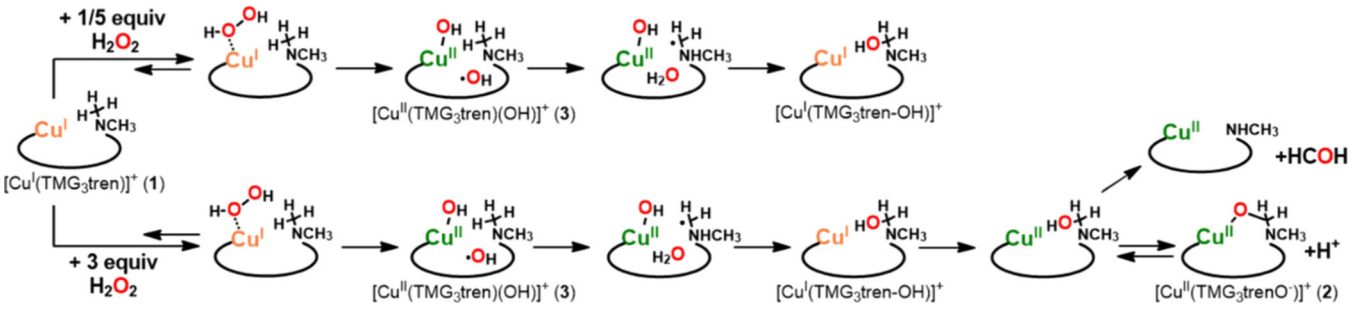

Scheme 5.

Proposed Courses of Reaction of $\left[Cu^{I}(TMG_3tren)\right]^{+}$(**1**) with Varying Amounts of H_2O_2[a]

[a] (Upper): **1**/H_2O_2 = 5 : 1 and the chemistry shown is for that one complex which reacts with H_2O_2 in a stoichiometric manner. (Lower): excess H_2O_2 relative to complex (**1**) produces the same hydroxylated ligand complex $Cu^{I}(TMG_3tren\text{-}OH)$; however the excess oxidant present leads to further chemistry (far right).

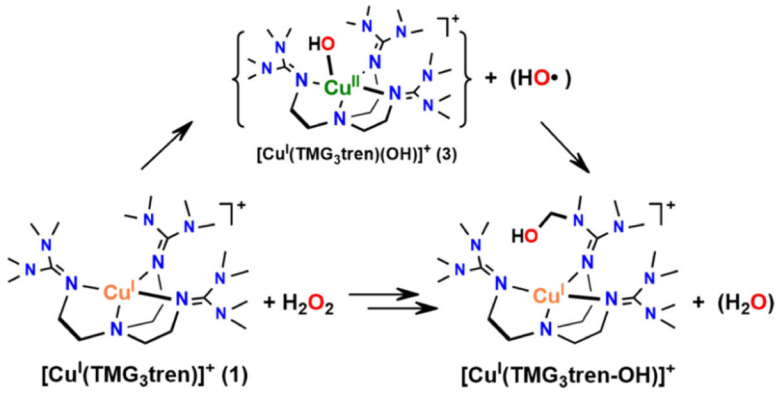

Scheme 2.

Complex $\left[Cu^{I}(TMG_{3}tren)\right]^{+}$(**1**) Reacts with Dry H_2O_2 to Afford Cu^{I} Complex Product Where a Ligand Methyl Group Has Been Hydroxylated, in Accordance with the Peroxygenase Pathway Postulated in LPMOs; See Text for Further Explanation